RSC Advances

ROYAL SOCIETY OF CHEMISTRY

www.rsc.org/advances

Cite this: DOI: 10.1039/c0xx00000x

www.rsc.org/xxxxxx

Communication

Acid-responsive nanospheres from an asparagine-derived amphiphile

Adelphe M. Mfuh,[a] Mathew P. D. Mahindaratne,[b] Audrey E. Yñigez-Gutierrez,[a] Juan R. Ramos Dominguez,[a] Jefferson T. Bedell II,[a] Carlos D. Garcia,[a] and George R. Negrete*[a]

We describe the synthesis and self-assembly of an asparagine-derived amphiphile. The self-assembled systems formulated with the inclusion of cholesterol (0-50 mol%) show encapsulation for a hydrophobic model drug and rapidly disintegrate in response to mild acidic conditions.

Amino acid derived amphiphiles and their related lipopeptides have attracted considerable attention for their use in the design and fabrication of nanostructures for advanced material development.[1] These entities undergo spontaneous self-organization into a number of discrete structures with varied aspect ratios. Some of these structures including micelles, vesicles, nanotubes, and nanogels have shown potential in the encapsulation of chemical agents and as a result, they are well-recognized as delivery vehicles for a variety of small bioactive molecules such as drugs, imaging agents, nucleic acids, and proteins.[2] The nano-encapsulation of these materials are reported to confer important pharmacological advantages including the protection of therapeutic materials from unwanted side effects, the enhancement of therapeutic efficacies through improved bioavailability,[3,4] and the exposure of these materials for longer periods of time at the desired location.[5,6] The ability to tune these systems in response to environmental stimulus has enabled the development of programmable controlled-release modalities for drug delivery applications.[7,8] Stimuli including pH,[9] redox,[10] light,[11] heat,[12] magnetism,[13] and enzymatic activity[14] have been employed as triggers to effect the dynamic release of inclusions at desired locations. Among these approaches, pH-mediated release is attractive because acidity is commonly associated with disease-relevant physiological processes including tumor growth, endosomal trafficking, and inflammation.[15] Notable pH-sensitive nanocarriers reported to date employ labor-intensive chemical modification of phospholipids and/or block copolymers with acid-cleavable or acid-responsive domains such as imines,[16] enol ethers,[17] and ortho esters.[18] In this manuscript, we report the first use of an *N,N*-acetal group as the pH responsive unit of the lipid nanoparticle formulation. Prior studies in our laboratory indicted that the *N,N*-acetal unit is readily assembled, stable to neutral conditions, and undergoes disassembly to its constituents under acidic conditions. These characteristics suggested this unit as a promising trigger mechanism for controlled release applications. Here, we disclose the synthesis and spontaneous self-assembly of an *N,N*-acetal-containing asparagine-derived amphiphile and its application in the formation of nanocarriers with pH-responsive release properties (Fig. 1).

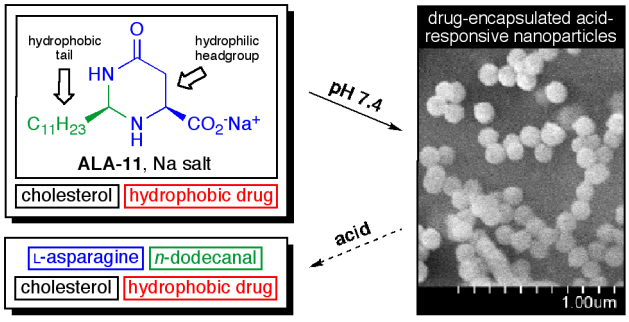

Fig. 1 Schematic representation of the pH-responsiveness of ALA-11.

The present pH-sensitive amphiphile comprised a negatively charged hydrophilic heterocycle carboxylate headgroup and a *single-chain* hydrophobic domain (ALA-11, Fig. 1) incorporated upon cyclocondensation of L-asparagine and dodecanal (Fig. 2A). This construct was previously prepared as an *unisolated* intermediate that was then acylated with stearoyl chloride to obtain an acid stable lipid ($ALA_{11,17}$).[19] We anticipated that the intermediate could be employed in a triggered-release nanoparticle (NP) since the lipid supported a linear alkyl chain for hydrophobic associations and was observed to degrade under acidic conditions (Fig. 1).

Lipid NPs generated from *single chain* fatty acids in combination with cholesterol have been shown to form lamellar liquid ordered (l_o) phases with thicker and less permeable membranes that are ideal for drug delivery.[20] The acid-triggered degradation of charged non-phospholipid nanocarriers are relatively rare in literature, and have recently been implemented with fatty analogues of amines[21] and acids.[22] Here we report tetrahydropyrimidinone-based amphiphile ALA-11 that is quantitatively prepared in one step (Fig. 2A) and its use in a new form of pH-responsive nanocarriers with cholesterol.

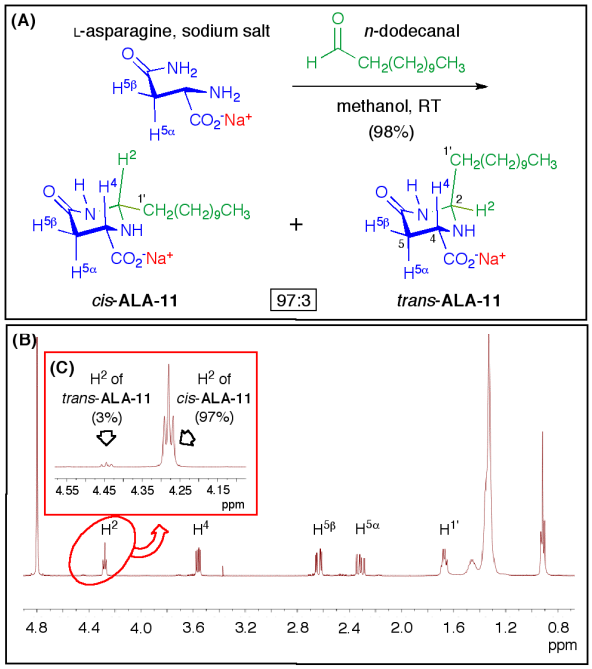

Fig. 2 (A) Synthesis of sodium (2*R*,4*S*)-6-oxo-2-undecyhexahydropyrimidine-4-carboxylate (ALA-11) and (B) the ^{1}H NMR spectrum of ALA-11 in D_2O exhibiting signals for the major and minor diastereomers (H^2-signal is illustrated in (C)).

An equimolar ratio of L-asparagine and *n*-dodecanal in methanolic NaOH (1.1 equiv) in ambient conditions generated ALA-11 in high yield (99%; S2, ESI†). Importantly, ALA-11 can be isolated in high purity by simply evaporating the solvent. The reaction afforded a mixture of *cis*-

and *trans*-hexahydropyrimidinones with pendant carboxylate and *n*-$C_{11}H_{23}$-groups. The major product was assigned the diequatorial 2,4-*cis*-isomer (*cis*-ALA-11; Fig. 2A) based on spectroscopic evidence[23] and prior precedent for the relative stereochemistry of aldehyde-asparagine cyclocondensates,[19,24] which have been ascribed to the expected thermodynamically preferred 1,3-diequatorial orientation of larger substituents in the ring closure step[25b] The equatorial assignment of the 4-CO_2^- group was unequivocally established by vicinal spin-spin coupling constants ($^3J_{4,5\alpha} \approx 12$ Hz, and $^3J_{4,5\beta} \approx 5$ Hz), in the ^{1}H NMR spectrum (Fig. 2B)[25a,b] In prior studies, the ^{1}H NMR H2 triplet of the major cis diastereomer consistently appeared upfield of the corresponding minor diastereomer signal.[25] Based on these patterns, the ^{1}H NMR signals at 4.3 and 4.5 ppm were assigned the H2 of *cis*- and *trans*-ALA-11, respectively, and the cis/trans mol ratio (97/3) was calculated based on the corresponding integrals (Fig. 2C).[26]

The formation of supramolecular assemblies by ALA-11 was investigated employing ^{1}H NMR spectroscopy, light scattering, scanning and transmission electron microscopies (SEM and TEM, respectively), and fluorescence studies. Thus, the influence of hydrophobicity on the formation and properties of ALA-11 self-assembled aggregates was explored by incorporating increasing amounts of cholesterol in the self-assembly. Various mixtures of the constituents were dissolved in 50/50 chloroform/methanol (vol/vol) followed by solvent evaporation to generate thin films. To study the influence of cholesterol on the aggregation of ALA-11 by ^{1}H NMR spectroscopy, the thin films were hydrated with deuterium oxide (D_2O) to afford cloudy suspensions. The ^{1}H NMR spectra (S6, ESI†) of the colloidal suspensions exhibited increasing signal broadening of the characteristic heterocyclic signals as the cholesterol content increases, which is indicative of the formation of supramolecular aggregates.[27] The respective morphologies of the cholesterol/ALA-11 system were revealed using scanning electron microscopy (SEM). The studies were performed on freshly prepared ALA-11 formulations consisting of increasing molar concentration of cholesterol, which were negatively stained with uranyl acetate (2% w/v; 2 drops) and analyzed by SEM. The micrographs showed homogenously dispersed nanospheres with mean diameter of ~150 nm (Fig. 3). Interestingly, the size of the nano-assemblies in SEM did not appear to be significantly affected by the amount of cholesterol. The particle sizes of the respective cholesterol/ALA-11 formulations obtained by dynamic light scattering (DLS) were larger than those obtained from SEM and the sizes increased for increasing cholesterol content.[13b] For instance, the average particle size determined by DLS for ALA-11 nanospheres without cholesterol was found to be 162 nm (S11B, ESI†).[28] The PDI values were not significantly different among the formulations studied. The surface charge densities (ζ), on the other hand, became significantly less negative at the highest cholesterol content (S11, ESI†). These results suggest the incremental displacement of ALA-11 (the charged component) in the NP as the amount of cholesterol increases, leading to diminished surface charge density and larger observed particle sizes.

To investigate the effect of cholesterol on the critical aggregation concentration (CAC), UV spectrophotometry was employed.[29] In these experiments, three formulations of cholesterol/ALA-11 (mol ratios of 0/100, 20/80, and 40/60) were prepared and their optical densities (ODs) at 400 nm were recorded. Aliquots from these samples were diluted with PBS (10 mM, pH 7.4, 137 mM NaCl, and 37 mM KCl) to generate a series of colloidal dispersions of known concentrations. The CACs were obtained from the intersecting straight-lines from the log/log plots of the OD versus concentration (S13, ESI†). The CACs for the neat ALA-11 formulation (0/100), and for the 20/80 and 40/60 cholesterol/ALA-11 formulations (0.34, 0.18, and 0.066 mM, respectively) decreased as the cholesterol content in the formulation increased. The relatively low CAC in these systems, compared to SDS for example (CMC = 7.9 mM),[30] may be associated to the formation of complementary headgroup hydrogen-bonding interactions in conjunction with increasing hydrophobic organizational effects with increasing cholesterol content.

Fluorescence experiments using Nile red (NR) were employed to monitor the effect of cholesterol on the micropolarity of the hydrophobic core of the ALA-11 NPs.[31] In these experiments, thin films composed of cholesterol/ALA-11 (0/100, 10/90, 20/80, 30/70, 40/60, and 50/50) and NR (0.15 mol%) were prepared in PBS (33 mM total lipid content). The unincorporated Nile red in these suspensions was removed by passage through 0.45 μm filters and aliquots (200 mL) were quantitatively diluted with PBS (2.8 mL). The emission spectrum for each formulation was obtained after excitation at λ 485 nm and the normalized fluorescence intensity was plotted versus the emission wavelengths (Fig. 4a). The samples exhibited decreased λ_{max} as cholesterol increased (Fig. 4a & 4b). The observed blue shift in the emission spectrum of NR (visual to the naked eye; Fig. 4c), a result of the diminished stabilization of the charge-separated excited states of the fluorophore, is characteristic of increased hydrophobicity in the particle core[32] as cholesterol increases. The blue shift in the emission spectra increases to a maximum at 40–50 mol% cholesterol, suggesting that the NPs internalize the higher portions of cholesterol and become more hydrophobic, at least up to 50 mol%.

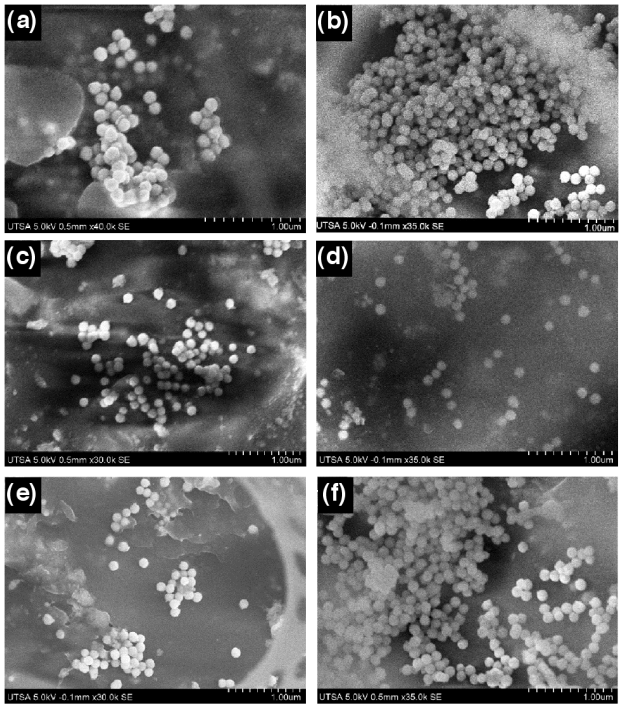

Fig. 3 Scanning electron micrographs of uranyl acetate-stained cholesterol/ALA-11 (mol/mol) formulations: (a) 0/100; (b) 10/90; (c) 20/80; (d) 30/70; (e) 40/60; and (f) 50/50.

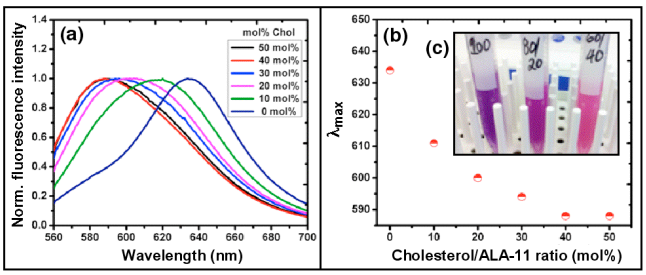

Fig. 4 (a) Plot of normalized fluorescence intensity of Nile red in different cholesterol/ALA-formulations in PBS at pH 7.4. (b) Plot of fluorescence emission spectra versus cholesterol content in ALA-11 nanoassembly. (c) Photograph showing the color differences of selected Nile red encapsulated cholesterol/ALA-11 nanocarrier formulations in (L to R): 0/100, 20/80, and 40/60 mol.

Transmission electron microscopy (TEM) was employed to observe a more detailed picture of the morphology of the NPs seen in SEM and also to determine if the observed nanostructures are hollow (liposomes) or solid lipid NPs.[33] In this experiment, a cholesterol/ALA-11 (40/60) dispersion prepared as described for the SEM studies was subjected to TEM analysis (S8, ESI†). The data depicts the presence of spherical liposomal nanostructures with dimensions comparable to those inferred from SEM (Fig. 3). In addition, micellar structures were also visualized.

Interestingly, some vesicles seen on TEM possess an inner and outer diameter of approximately 80 and 130 nm, respectively, corresponding to an average membrane thickness of approximately 44 nm, which suggests the presence of multilayered structures.

We investigated the ability of the cholesterol/ALA-11 NPs to efficiently encapsulate hydrophobic drugs using the dimethyl ester of protoporphyrin IX (PPIX-Me_2), which has excellent potential as a photodynamic therapy (PDT) sensitizer but exhibits poor bioavailability due to insolubility.[34] Following procedures used in the encapsulation of Nile red, PPIX-Me_2 (2 mol%) was introduced into cholesterol/ALA-11 nanospheres and the unincorporated PPIX-Me_2 was removed upon passage through either a 0.45 μm filter or a Sephadex G-75 column. The fluorescence emission spectra of these samples were obtained (λ_{ex} 400 nm and λ_{em} 630 nm) before and after filtration (S16 & S17, ESI†), and the encapsulation efficiencies were estimated from the ratio of the emission maxima. The results of the samples passed through 0.45 μm filters showed that the encapsulation efficiencies of freshly prepared 0/100, 20/80, and 40/60 cholesterol/ALA-11 formulations were 57, 82, and 65% (or 21, 31, and 26 μg/mg of lipids), respectively (Gray bars; S18, ESI†). In comparison, encapsulation efficiencies of the freshly prepared samples of 20/80 and 40/60 cholesterol/ALA-11 formulations following gel filtration (Sephadex G-75) were found to be 79 and 67% (or 30 and 27 μg/mg of lipids), respectively (S17, ESI†), and are in good agreement with the encapsulations recorded from dialysis filtrations. These results indicate that either method may be used to remove unincorporated material. Interestingly, the encapsulation efficiency of the 20/80 cholesterol/ALA-11 formulation was higher compared to the encapsulation of the 40/60. This observation is consistent with a diminished hydrophobic capacity caused by the presence of the extra cholesterol in the later formulation. After storage at room temperature for two weeks, the encapsulation efficiencies of the respective formulations decreased to 27, 78, and 60% (or 10, 29, and 24 μg/mg of lipids), respectively (Black bars; S18, ESI†). The small loss of encapsulated dye from the formations with greater cholesterol content demonstrates that cholesterol plays an important role in the stability of the respective encapsulated formulations.

The presence of the acid-labile *N,N*-acetal function on the headgroup of ALA-11 lipid was designed to impart pH-sensitivity to this system. Thus, the pH-dependent degradation behavior of the lipid in aqueous dispersions was examined by *UV-vis* and ^{1}H NMR experiments. The *UV-vis* experiment is based on the acid degradation of the lipid to dodecanal, which increases turbidity upon precipitation in water. Briefly, a thin film of ALA-11 lipid was dispersed in PBS (pH 7.4) to make a 33 mM lipid dispersion. Aliquots of the dispersion (200 μL) were further diluted with phosphate or acetate buffer concentrations (3 mL at pH 5.0, 6.0, and 7.4). The optical densities of the formulations at 400 nm were obtained and plotted versus time for each of the samples. The results show that the degradation of ALA-11 at pH 5.0 (Fig. 5a & 5b) was almost complete within 8 to 10 min ($t_{1/2} \approx 4$ min). At pH 6.0 the degradation was slower such that completion was observed at 250 min ($t_{1/2} \approx 100$ min). And at pH 7.4, no significant degradation was observed during the 4 hour experiment time. To complement these studies, ^{1}H NMR spectroscopy was employed to monitor the time-dependent depletion of the heterocyclic moiety of the lipid. Deuterated formulations of ALA-11 in a phosphate buffer at *pD* 7.8 (pH 7.4; 33 mM) were further diluted and the initial ^{1}H NMR spectrum was recorded immediately, and additional spectra were collected at 10 min intervals. The results are presented as a plot of the percent decrease of the H2 proton versus time (S21, ESI†). At *pD* 5.4 (pH 5.0), the hydrolysis of the heterocycle was completed before the initial spectrum could be obtained, indicating very rapid decomposition. At *pD* 6.4 (pH 6.0) the degradation was slowly progressed and completed after approximately 240 min (S21a & S21b). As expected, there was no significant change in the heterocycle at *pD* 7.8 over the 4 h of data collection (S21c & S21d). These results are in good agreement with the data obtained by optical density measurements (Fig. 5). Attempts to study the decomposition of the ALA-11 NPs comprised with cholesterol by ^{1}H NMR were unsuccessful due to the presence of significant peak broadening in the spectra. It should be noted that after prolonged storage at room temperature (2 months) the NMR samples developed significant turbidity, suggesting that the NPs are incompatible with prolonged storage.

The ability of selected cholesterol/ALA-11 self-assembly formulations (0 and 40 mol% cholesterol) to retain or associate with Nile red (NR) was monitored spectrofluorimetrically in selected pH media (pH 7.4, 6.0, and 5.0). NR fluorescence is known to become quenched in aqueous media. For the sample without cholesterol at pH 5.0, a rapid fluorescence decrease was observed, indicating the fast release of NR (blue diamonds; Fig. 6). In the presence of 40% cholesterol, however, rate of fluorescence decrease at same pH indicated that the dye release was significantly slowed, requiring 65 min for completion (blue triangles). The near complete release of NR at pH 6.0 occurred after 230 and 335 min for 0/100 and 40/60 mol ratios of cholesterol/ALA-11 formulations (red circles and green squares), respectively. The results of the NR release experiments on 0/100 cholesterol/ALA-11 formulation at pH 5.0 and 6.0 are in good agreement with those of optical density measurements at 400 nm (*c.f.*, Fig. 5 and S21, ESI†). At pH 7.4, there was no significant release of NR from either system for an extended time (~4 h). These data show that the pH-responsiveness of the ALA-11 nanocarrier system can be modulated by cholesterol content for the short-term, pH-responsive release of hydrophobic compounds.[20,21]

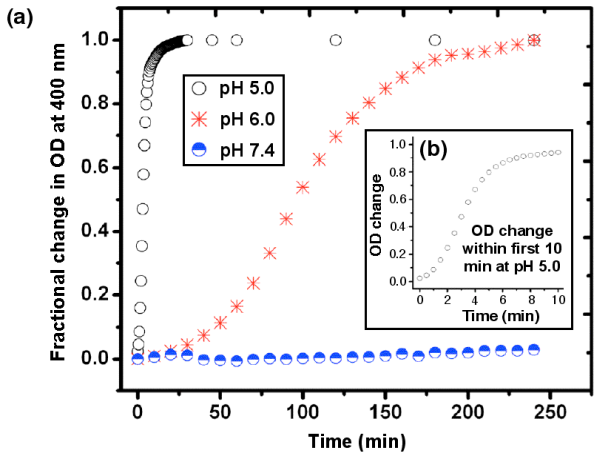

Fig. 5 (a) A plot of fractional change in optical density (OD) at 400 nm versus time showing the hydrolysis of ALA-11 at different pH. Insert (b) shows the expanded version of OD at 400 nm vs time at pH 5. These data are based on an increase in turbidity (optical density at 400 nm) during the course of the hydrolysis of the asparagine-derived amphiphile.

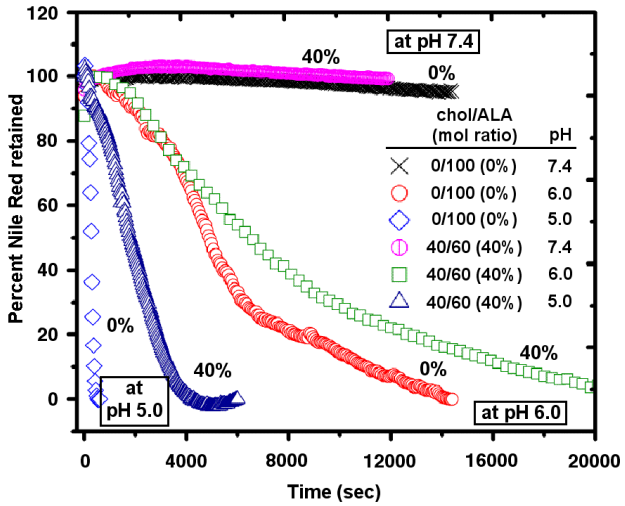

Fig. 6 A plot of percentage Nile red (NR) retained under various pH conditions as a function of time in selected cholesterol/ALA-11 formulations. The graphs show a rapid release of NR at pH 5.0, which becomes reduced in the presence of cholesterol. At pH 7.4, an insignificant release of NR was observed for both formulations.

The NPs described in this paper invite comparison to the work on nonphospholipid liposomes from several laboratories and on acid-degradable lipids that trigger NP content release from NPs. The palmitic acid/cholesterol NPs of Lafluer[20a,b] are stable at pH 5.5, below which content release occurs upon fatty acid protonation and physical separation from cholesterol. The ALA-11/cholesterol NPs undergo aminal decomposition and concomitant encapsulate release under mildly acidic conditions (pH 6). The aminal trigger is related to the thioamide,[9b] orthoester,[18] and enol ether[17] triggers, which also function by degrading the linkage between the polar headgroup and the lipid tail. The quantitative preparation, facile purification, and high structural purity are attractive features afforded by the present system. Also, the ALA-11 heterocycle headgroup may contribute to stabilizing the NPs above pH 7 via hydrogen bonding and ionic interactions at the water interface. Though the stabilities of these NPs have yet to be examined in drug delivery conditions, the rapid release of dye under mild acid conditions suggests its potential in drug delivery elicited by the ischemic physiology of tumor microenvironments.[35] In contrast to the pH-triggered drug delivery systems mentioned above, the solvatochromic and PPIX-Me_2 encapsulation studies in this work establish the suitability of this system for the hydrophobic drug delivery. Research in progress aims to improve the stability of this NP while maintaining the mild acid fragility.

In conclusion, a novel asparagine-derived lipid was prepared and shown to be self-assembled both as a neat lipid and in formulations containing cholesterol. The morphological integrity of the system did not appear to be significantly affected with the incorporation of up to 50 mol% cholesterol. Nile red solvatochromic studies showed significant differences in the micropolarity of the hydrophobic core of the system as the cholesterol in the formulations increases. Controlled release studies demonstrated a pH dependent degradation and release of hydrophobic NR. These studies also show that cholesterol significantly decreases the degradation rates of these assemblies in acidic environments. Thus, this system or its variants may find application in pH-responsive controlled release of hydrophobic drugs at mildly acidic locations such tumor cells. It is also important to emphasize that the degradation byproducts of ALA-11 carrier system, L-asparagine, *n*-dodecanal, and cholesterol, are nontoxic[36,37] and are thus unlikely to present hazards if employed as NPs for drug delivery.

We are grateful for funds provided the San Antonio Life Sciences Institute (SALSI) for these studies. We gratefully acknowledge Dr. Miguel Yacaman and Dr. Arturo Ponce-Pedraza (Department of Physics and Astronomy) for assistance with SEM and TEM, and the National Center for Research Resources (5 G12RR013646-12) and the NIH National Institute on Minority Health and Health Disparities (G12MD007591). We appreciate the technical contributions from Dr. Lorenzo Brancaleon, Dr. Mark Penick, and Mr. Djan Baffoe.

Notes and references

[a] *Department of Chemistry, University of Texas at San Antonio, One UTSA Circle, San Antonio, TX 78249-1644, USA.*

[b] *Texas A&M University-San Antonio, One University Way, San Antonio, TX 78224, USA.*

* Corresponding Author Phone: (210) 458-5448. Fax: (210) 458-7428. E-mail: george.negrete@utsa.edu.

† Electronic Supplementary Information (ESI) available: Experimental procedures and spectroscopy data. See DOI:10.1039/b000000x/

1 (a) S. Vauthey, S. Santoso, H. Gong, N. Watson and S. Zhang, *Proc. Natl. Acad. Sci. U.S.A.*, 2002, **99**, 5355–5360; (b) P. Koley and A. Pramanik, *Adv. Funct. Mater*, 2011, **21**, 4126–4136; (c) H. Sakai, K. Watanabe, Y. Asanomi, Y. Kobayashi, Y. Chuman, L. Shi, T. Masuda, T. Wyttenbach, M. T. Bowers, K. Uosaki and K. Sakaguchi, *Adv. Funct. Mater.*, 2013, **23**, 4881–4887; (c) S. Ghosh, B. Ambade and A. Ray, *Sci. Adv. Mater.*, 2013, **5**, 1837–1846.

2 P. Gao, *Mol. Pharm.*, 2008, **5**, 903–904.

3 Z. Gao, A. N. Lukyanov, A. Singhal and V. P. Torchilin, *Nano Lett.*, 2002, **2**, 979–982.

4 L. O. Cinteza, T. Y. Ohulchanskyy, Y. Sahoo, E. J. Bergey, R. K. Pandey and P. N. Prasad, *Mol. Pharm.*, 2006, **3**, 415–423.

5 L. Zhu, P. Kate and V. P. Torchilin, *ACS Nano*, 2012, **6**, 3491–3498.

6 P. Sanpui, A. Chattopadhyay and S. S. Ghosh, *ACS Appl. Mater. Interfaces*, 2011, **3**, 218–228.

7 C. M. Valmikinathan, S. Defroda and X. Yu, *Biomacromolecules*, 2009, **10**, 1084–1089.

8 P. D. Thornton and A. Heise, *J. Am. Chem. Soc.*, 2010, **132**, 2024–2028.

9 (a) D. Pornpattananangkul, S. Olson, S. Aryal, M. Sartor, C.-M. Huang, K. Vecchio and L. Zhang, *ACS Nano*, 2010, **4**, 1935–1942; (b) J. Connor and L. Huang, *Cancer Res.*, 1986, **46**, 3431–3435; (c) J. J. Sudimack, W. Guo, W. Tjarks and R. J. Lee, *Biochim. Biophys. Acta*, 2002, **1564**, 31–37.

10 W. Ong, Y. Yang, A. C. Cruciano and R. L. McCarley, *J. Am. Chem. Soc.*, 2008, **130**, 14739–14744.

11 Y. Wan, J. K. Angleson and A. G. Kutateladze, *J. Am. Chem. Soc.*, 2002, **124**, 5610–5611.

12 T. Kaiden, E. Yuba, A. Harada, Y. Sakanishi and K. Kono, *Bioconjugate Chem.*, 2011, **22**, 1909–1915.

13 (a) K. Katagiri, M. Nakamura and K. Koumoto, *ACS Appl. Mater. Interfaces*, 2010, **2**, 768–773; (b) L.-P. Tseng, H.-J. Liang, T.-W. Chung, Y.-Y. Huang, D.-Z. Liu, *J. Med. Biol. Eng.*, 2007, **27**, 29–34.

14 Y. Xing, C. Wang, P. Han, Z. Wang and X. Zhang, *Langmuir*, 2012, **28**, 6032–6036.

15 (a) X. L. Wu, J. H. Kim, H. Koo, S. M. Bae, H. Shin, M. S. Kim, B.-H. Lee, R.-W. Park, I.-S. Kim, K. Choi, I. C. Kwon, K. Kim and D. S. Lee, *Bioconjugate Chem.*, 2010, **21**, 208–213; (b) X.-Z. Yang, J.-Z. Du, S. Dou, C.-Q. Mao, H.-Y. Long and J. Wang, *ACS Nano*, 2012, **6**, 771–781.

16 X. Cai, C. Dong, H. Dong, G. Wang, G. M. Pauletti, X. Pan, H. Wen, I. Mehl, Y. Li and D. Shi, *Biomacromolecules*, 2012, **13**, 1024–1034.

17 J. A. Boomer, M. M. Qualls, H. D. Inerowicz, R. H. Haynes, V. S. Patri, J.-M. Kim and D. H. Thompson, *Bioconjugate Chem.*, 2009, **20**, 47–59.

18 Z. Huang, X. Guo, W. Li, J. A. MacKay and F. C. Szoka, Jr., *J. Am. Chem. Soc.*, 2006, **128**, 60–61.

19 A. M. Mfuh, M. P. D. Mahindaratne, M. V. Quintero, F. J. Lakner, A. Bao, B. A. Goins, W. T. Phillips and G. R. Negrete, *Langmuir*, 2011, **27**, 4447–4455.

20 (a) C. Paré and M. Lafleur, *Langmuir*, 2001, **17**, 5587–5594; (b) J. Ouimet, S. Croft, C. Paré, J. Katsaras and M. Lafleur, *Langmuir*, 2003, **19**, 1089–1097; (c) D. L. Gater, J. M. Seddon and R. V. Law, *Soft Matter*, 2008, **4**, 263–267.

21 Z.-K. Cui, A. Bouisse, N. Cottenye and M. Lafleur, *Langmuir*, 2012, **28**, 13668–13674.

22 T. Phoeung, P. Aubron, G. Rydzek and M. Lafleur, *Langmuir*, 2010, **26**, 12769–12776.

23 (a) M. J. Minch, *Concepts Magn. Reson.*, 1994, **6**, 41–56; (b) R. B. Nazarski and S. Leśniak, *Bull. Pol. Acad. Sci.-Chem.*, 2000, **48**, 19–25; (c) A. Thangamani, J. Jayabharathi and A. Manimekalai, *J. Chem. Sci.*, 2010, **122**, 579–586.

24 For 1,3-*cis*-stereochemistry of the major product see: (a) K. S. Chu, G. R. Negrete, J. P. Konopelski, F. J. Lakner, N. T. Woo and M. M. Olmstead, *J. Am. Chem. Soc.*, 1992, **114**, 1800–1812; (b) E. Juaristi,

D. Quintana, M. Balderas and E. García-Pérez, *Tetrahedron Asymmetry*, 1996, **7**, 2233–2246; (c) E. Juaristi, H. López-Ruiz, D. Madrigal, Y. Ramírez-Quiróz and J. Escalante, *J. Org. Chem.*, 1998, **63**, 4706–4710.

25 (a) F. J. Lakner and G. R. Negrete, *Synlett*, 2002, 643–645; (b) M. P. D. Mahindaratne, B. A. Quiñones, A. Recio III, E. A. Rodriguez, F. J. Lakner and G. R. Negrete, *Tetrahedron*, 2005, **61**, 9495–9501; (c) M. P. D. Mahindaratne, B. A. Quiñones, A. Recio III, E. A. Rodriguez, F. J. Lakner and G. R. Negrete, *ARKIVOC*, 2005, **6**, 321–328.

26 The cis/trans ratio of 2-*tert*-butylhexahydropyrimidine-6-one-4-carboxylic acid (the C2-substitution is *tert*-butyl group instead of *n*-undecyl) obtained from the similar cyclo-condensation was reported as 86/14 for its potassium salt (reference 25a and b).

27 J. Liu, Y. Pang, W. Huang, X. Zhu, Y. Zhou and D. Yan, *Biomaterials*, 2010, **31**, 1334–1341.

28 X. Liang, G. Mao and K. Y. S. Ng, *J. Colloid Interface Sci.*, 2004, **278,** 53–62.

29 P. Debye, *J. Phys. Chem.*, 1949, **53**, 1–8.

30 M. R. Beccia, T. Biver, B. García, J. M. Leal, F. Secco, R. Ruiz and M. Venturini, *Dalton Trans.*, 2012, **41**, 7372–7381.

31 Benzo[*a*]phenoxazine type fluorophore: (a) P. J. G. Coutinho, in *Reviews in Fluorescence 2007*, ed. C. D. Geddes, Springer Science+Business Media, LLC, New York, NY, 2009, vol. 4, ch. 14, pp. 335–362. (b) P. Greenspan and S. D. Fowler, *J. Lipid Res.*, 1985, **26**, 781–789.

32 M. B. Moshe, S. Magdassi, Y. Cohen and L. Avram, *J. Colloid Interface Sci*., 2004, **276**, 221–226.

33 A. zur Mühlen, C. Schwarz and W. Mehnert, *Eur. J. Pharm. Biopharm*., 1998, **45**, 149–155.

34 E. D. Sternberg, D. Dolphin and C. Brückner, *Tetrahedron*, 1998, **54**, 4151–4202.

35 L. E. Gerweck, *Seminars in Radiation Oncology*, 1998, **8**, 176–182; P. Vaupel, *Seminars in Radiation Oncology*, 2003, **14**, 198–206.

36 a) L-Asparagine is listed as an existing food additive: M. Yokohira, K. Hosokawa, K. Yamakawa, N. Hashimoto, S. Suzuki, Y. Matsuda, K. Saoo, T. Kuno and K. Imaida, *Food Chem. Toxicol.*, 2008, **46**, 2568–2572; (b) The acute oral LD50 of *n*-dodecanal (lauraldehyde) in rats is 23.1 g/kg: R. Tisserand and R. Young, in *Essential Oil Safety*, Churchill-Livingstone-Elsevier (Elsevier's Health Sciences Division), Philadelphia, PA, 2nd Ed., 2014, ch. 14, p. 550.

37 Fatty aldehyde dehydrogenase (EC 1.2.1.48) in Human liver converts long-chain fatty aldehydes to their corresponding acids (M. A. Keller, K. Watschinger, G. Golderer, M. Maglione, B. Sarg, H. H. Lindner, G. Werner-Felmayer, A. Terrinoni, R. J. A. Wanders and E. R. Werner, *J. Lipid Res.*, 2010, **51**, 1554–1559). Thus, EC 1.2.1.48 would convert dodecanal to the corresponding acid dodecanoic acid, which is a component of triglycerides and comprises about half of the fatty acid content in coconut oil (44.6%), babassu fat (40-55%), and palm kernel oil (45-55%), all of which are parts of human food chain (J. Beare-Rogers, A. Dieffenbacher and J. V. Holm, *Pure Appl. Chem.*, 2001, **73**, 685–744).